nature neuroscience

Gene expression changes and molecular pathways mediating activity-dependent plasticity in visual cortex

Daniela Tropea[1], Gabriel Kreiman[2], Alvin Lyckman[1,3], Sayan Mukherjee[2,3], Hongbo Yu[1], Sam Horng[1] & Mriganka Sur[1]

Two key models for examining activity-dependent development of primary visual cortex (V1) involve either reduction of activity in both eyes via dark-rearing (DR) or imbalance of activity between the two eyes via monocular deprivation (MD). Combining DNA microarray analysis with computational approaches, RT-PCR, immunohistochemistry and physiological imaging, we find that DR leads to (i) upregulation of genes subserving synaptic transmission and electrical activity, consistent with a coordinated response of cortical neurons to reduction of visual drive, and (ii) downregulation of parvalbumin expression, implicating parvalbumin-expressing interneurons as underlying the delay in cortical maturation after DR. MD partially activates homeostatic mechanisms but differentially upregulates molecular pathways related to growth factors and neuronal degeneration, consistent with reorganization of connections after MD. Expression of a binding protein of insulin-like growth factor-1 (IGF1) is highly upregulated after MD, and exogenous application of IGF1 prevents the physiological effects of MD on ocular dominance plasticity examined *in vivo*.

Alteration of visual input during postnatal development causes adaptive changes in the maturation of visual cortex circuitry[1]. However, the mechanisms underlying functional and structural changes in the cortex resulting from activity remain unresolved. A common protocol for examining mechanisms of activity-dependent plasticity is to alter visual experience during a critical period of development[2]. One way by which the role of activity in visual cortical development has been assessed is by raising animals in complete darkness from birth. Dark rearing (DR) alters synaptic strength[3] and structure[4], changes the threshold for eliciting synaptic potentiation and depression[5] and prolongs the critical period for eliciting experience-dependent changes in visual function[6]. The effects of DR are consistent with the proposal that a reduction of afferent drive alters the maturation of inhibition in cortex[7] and in the longer term upregulates synaptic efficacy and intracellular signaling owing to a homeostatic regulation of inputs by cortical neurons[8]. The molecular substrates of these functional effects are unknown.

A different manipulation that leads to unbalanced activity between the two eyes is monocular deprivation (MD). Suturing shut the lids of one eye during the critical period causes an increase in the proportion of neurons in the binocular part of V1 that respond to the open eye[9]. Short-term MD causes reorganization of intracortical connections both functionally and structurally[10–12], whereas long-term MD leads in addition to a reduction of thalamocortical arbors from the deprived eye and an expansion of arbors from the non-deprived eye[13]. Several studies have examined the effects of specific molecules on ocular dominance plasticity mediated by MD, aiming at understanding the synaptic changes that accompany MD[2]. Indeed, some of the physiological effects of monocular activity blockade, particularly in the monocular segment, resemble the homeostatic effects of DR[3]. However, the structural effects of long-term MD are likely to be mediated by additional molecules, including some distinct from those used to target eye-specific projections to V1 during development[14]. The identity of such molecules and how they are regulated by MD is unknown.

Although some of the molecules in visual cortex associated with the critical period for ocular dominance plasticity have been examined[15,16], there are no data on sets of genes that are up- or downregulated in different paradigms of activity-dependent plasticity or on the molecular links between development under different forms of visual experience. We used DNA microarrays to examine large-scale changes in gene expression in V1 after DR and MD, using quantitative analyses of single genes as well as computational analyses of gene sets. On the basis of these results, we performed semiquantitative PCR assays for a wide range of cDNAs of V1-expressed genes and compared the data to those from the microarrays. We further examined the expression of key molecules through immunohistochemistry. We found that DR specifically downregulates parvalbumin, a marker for a subset of inhibitory neurons in the cortex. Furthermore, the two forms of visual deprivation invoke similar but distinct responses in V1: a homeostatic response after DR that upregulates a wide array of genes involved in synaptic transmission and electrical activity, and an additional response after MD that is consistent with the withdrawal of deprived eye inputs and the expansion of non-deprived eye inputs. The findings indicate that a

[1]Department of Brain and Cognitive Sciences and Picower Institute for Learning and Memory and [2]Department of Brain and Cognitive Sciences and McGovern Institute for Brain Research, Massachusetts Institute of Technology, Cambridge, Massachusetts 02139, USA. [3]Present addresses: Tufts School of Medicine, Caritas St. Elizabeth's Medical Center, Center for Biomedical Research 406, 736 Cambridge Street, Brighton, Massachusetts 02135-2997, USA (A.L.); Institute for Genome Sciences and Policy, CIEMAS, Duke University, 101 Science Drive, Box 3382, Durham, North Carolina 27708, USA (S.M.). Correspondence should be addressed to M.S. (msur@mit.edu).

Received 17 February; accepted 28 March; published online 23 April 2006; doi:10.1038/nn1689

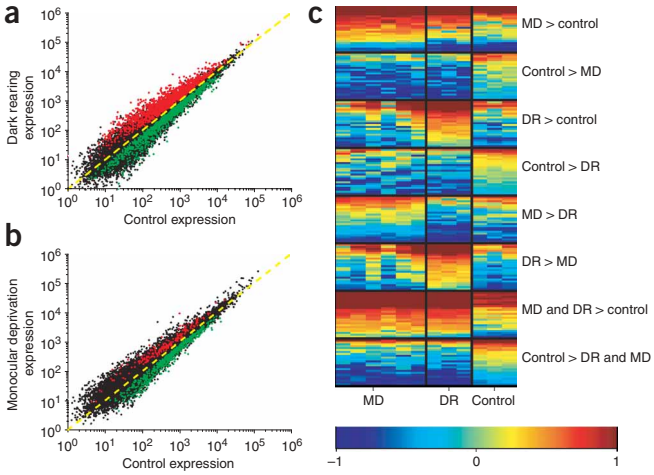

Figure 1 Analysis and characterization of genes activated by different protocols of visual input deprivation. Three experimental groups were considered: control mice, dark-reared (DR) mice and monocularly deprived (MD) mice. From each sample, tissue from primary visual cortex (V1) was taken at P27. (**a**,**b**) Comparison of gene expression in (**a**) dark-reared versus control and (**b**) monocularly deprived versus control mice, showing the expression levels of all probes. Gene expression is shown on a logarithmic scale. Genes showing expression levels significantly different from control ($P \leq 0.01$) are shown in red (overexpression in deprivation protocol) or in green (underexpression). (**c**) Heat map providing overview of representative genes that showed differential expression after visual deprivation ($P \leq 0.01$). Each column corresponds to a separate sample ($n = 6$ for MD, $n = 3$ for DR and $n = 3$ for control). Brilliant red corresponds to high expression and dark blue to low expression (see color scale at bottom). For each group, 25 randomly chosen genes among the significant genes are shown here. Genes within each group are sorted on the basis of their expression values.

pathway not previously implicated in activity-dependent plasticity in visual cortex, the IGF1 pathway, has a key role in ocular dominance plasticity. By using optical imaging of intrinsic signals combined with exogenous application of IGF1, we showed that addition of IGF1 prevents the shift in ocular dominance following MD. Analysis of IGF1 action using both microarrays and protein immunohistochemistry suggests that this growth factor exerts its role by modulating the expression of phosphatidylinositol 3-kinase (PI3K).

RESULTS

Changes in gene expression after DR and MD

The mice used for microarray analyses of long-term visual deprivation were (i) DR mice reared in complete darkness from birth till postnatal day (P) 27, the peak of the critical period for ocular dominance plasticity in mice[17]; (ii) MD mice that had one eyelid sutured from before eye-opening (at P11–12) through P27; and (iii) P27 control mice, reared under standard conditions. V1 was identified by stereotaxic coordinates and its location confirmed both by optical imaging of intrinsic signals and by injections that retrogradely labeled cells in the lateral geniculate nucleus (LGN)[18]. RNA was extracted from V1 and hybridized to microarrays. First, we compared the expression level of gene transcripts between control and deprived mice (**Fig. 1**) using a significance analysis of microarrays procedure (**Supplementary Methods** online). We thus obtained two lists of genes for each deprivation protocol: those that were upregulated in the deprived conditions as compared to control (1,930 genes: 1,730 genes upregulated after DR and 200 genes upregulated after MD) and those that were downregulated in the deprived conditions as compared to control (1,381 genes: 950 genes downregulated after DR and 431 genes downregulated after MD). The complete list of significantly ($P < 0.01$) up- and downregulated genes is reported in tables for each experiment at the website http://web.mit.edu/msur/www/Tropea.html.

We used the Gene Ontology (GO) database (**Supplementary Methods**) to group differentially expressed genes according to the biological processes in which their products are involved. Of the 3,311 genes differentially expressed in visually deprived groups, 1,227 encode proteins that have known functions and have been reported in GO categories (level 3) for general biological processes. This analysis showed that some biological processes are common to both deprivation conditions, whereas others are differentially, or even exclusively, represented in one condition or the other (**Supplementary Table 1** online). To analyze the distinction further, we carried out a more detailed examination of genes encoding glutamatergic and GABA receptors, including specific subunits (**Table 1** and **Supplementary Fig. 1** online). This comparison of the main forms of excitatory and inhibitory transmission in the cortex showed that none of these receptor genes was downregulated, whereas a substantial set of genes was upregulated, after the two forms of deprivation. The effect was greater after DR than after MD (**Fig. 2a**).

Several studies have reported that DR induces a delay in the maturation of inhibition[6,7] . We found no change in GAD65 expression after DR or MD, but an increase in GAD67 expression after DR (**Fig. 2b**). More generally, we found a reduction in expression of only

Table 1 Changes in expression of genes encoding GABA subunits and glutamate receptors after MD and DR

Receptor	MD	DR
GluR1	=	+
GluR2	+	+
GluR3	+	+
NMDA1	=	+
NMDA2A	=	+
NMDA2B	=	+
NMDA2C	=	=
NMDA2D	=	=
mGluR3	=	=
mGluR5	=	=
mGluR8	=	=
$GABA_A$ α1	=	+
$GABA_A$ α2	+	+
$GABA_A$ α3	+	+
$GABA_A$ α4	=	+
$GABA_A$ α6	+	=
$GABA_A$ β1	+	+
$GABA_A$ β2	=	+
$GABA_A$ β3	+	+
$GABA_A$ γ1	=	=
$GABA_A$ γ2	=	+
$GABA_A$ γ3	=	=
$GABA_A$ δ	=	=
$GABA_A$ ε	=	=
$GABA_B$ 1	=	=
$GABA_C$ ρ1	=	=
$GABA_C$ ρ2	=	=

+, significant ($P \leq 0.05$) increase in the mRNA level in the deprived condition relative to control; =, no significant change. No gene was downregulated after deprivation relative to control.

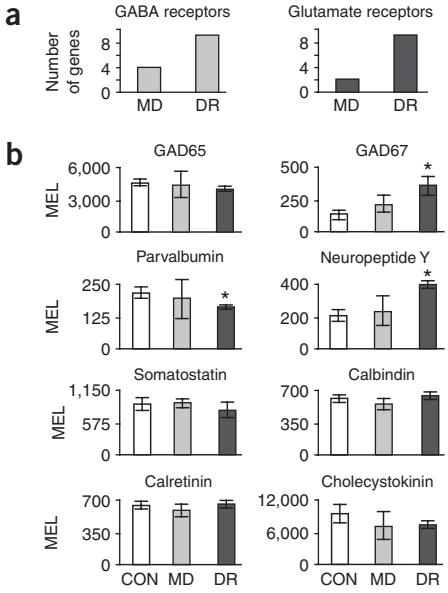

Figure 2 Regulation of genes involved in excitatory and inhibitory transmission after MD and DR. (**a**) Numbers of GABA and glutamate receptor genes that were significantly upregulated after MD or DR versus control. No genes were downregulated. See **Table 1** and **Supplementary Figure 1** for more information. (**b**) Microarray expression levels (MEL) in control (CON), MD and DR mice of genes encoding glutamic acid decarboxylase (GAD65 and GAD67), the synthetic enzymes for GABA, and several markers of different classes of inhibitory interneurons. Only the probes for parvalbumin were significantly downregulated after DR, whereas those for the other markers were either upregulated or unchanged. Error bars indicate s.e.m. Star indicates a significant change ($P < 0.05$, two-tailed *t*-test).

one gene associated with cortical inhibitory neurons: all the probes associated with parvalbumin were downregulated after DR, whereas probes associated with other markers of inhibitory neurons[19], including calbindin, somatostatin, calretinin, cholecystokinin and neuropeptide Y, were either upregulated or did not change after DR (**Fig. 2b**). There was no change in any of these markers after MD (see also discussion below and **Supplementary Fig. 2** online). Thus, specific functional consequences of DR are possibly mediated by a reduction in the number of neurons expressing parvalbumin.

Next, we compared the microarray expression levels of a subset of genes (**Fig. 3a**) with results from an independent measure of gene expression using semiquantitative RT-PCR performed on samples independent from those used for microarrays. The genes selected were significantly upregulated ($P < 0.05$) in DR or MD cortex as compared to control, with at least a 1.5-fold greater expression after one or other form of deprivation (the list of genes tested for RT-PCR included both up- and downregulated genes and is available on the website; data for downregulated genes are not shown in **Fig. 3**). RT-PCR analysis confirmed the microarray analysis in over 80% of instances (21 of 25 genes after DR and 22 of 25 genes after MD). We examined representative genes that were upregulated after DR alone, after MD alone or after both (**Fig. 3b,c**). Genes upregulated after DR (but not MD) in the microarray data included ones encoding molecules associated with synaptic structure and function, such as those involved in synapse formation (neurexin-1 and synapsin-2), synaptic transmission mechanisms such as exocytosis (synaptotagmin-1), neurotransmitter receptors (glutamate receptor-1 (GluR1)) and calcium-activated signaling (calmodulin-dependent protein kinase IIα (CaMKIIα) and cAMP response element–binding protein (CREB)). The changes observed through RT-PCR were consistent with the observations from the microarray data. That is, we found an increase in the expression of these molecules in the DR cortex, and there was a greater increase in the DR condition compared to MD for each of them.

Fewer genes were upregulated after MD (but not DR) than in controls and, notably, they included genes encoding proteins that are usually implicated in cellular pathology, including carcinogenesis (the DEAD-box RNA helicase Ddx6[20]) and degeneration (signal transducer and activator of transcription-1 (STAT1); see below), or are activated by seizure (CaMKIIδ[21]). These genes also showed greater expression in the RT-PCR analysis (**Fig. 3c**). Finally, genes that were upregulated after both DR and MD included those encoding molecules associated with synaptic activity (GluR3 and $GABA_A$ α2) as well as molecules associated with neuronal growth and reorganization of connections (insulin-like growth factor binding protein-5 (IGFBP5); see below) and aspects of brain development (nuclear factor IB (Nfib)[22]). Overall, these data suggest increased activation of a wide range of synaptic and neuronal mechanisms in V1 of DR mice, and to a lesser extent in MD mice, compared to control mice. Conversely, they suggest an increased activation of neuronal growth and degeneration mechanisms in MD mice, and to a lesser extent in DR mice, compared to control mice.

Although the effects of MD are pronounced in the long term, they are also significant in the short term[10–12]. To examine similarities and differences with the long (16 d) period of MD, we carried out a microarray analysis of a short (4 d) period of MD, from P23–27. Notably, short-term MD led to changes in the expression of many more genes than long-term MD (**Supplementary Fig. 2** and **Supplementary Table 2** online). About 50% of the genes that were up- or downregulated after long-term MD were also altered in expression after short-term MD; the upregulated genes included those encoding Ddx6,

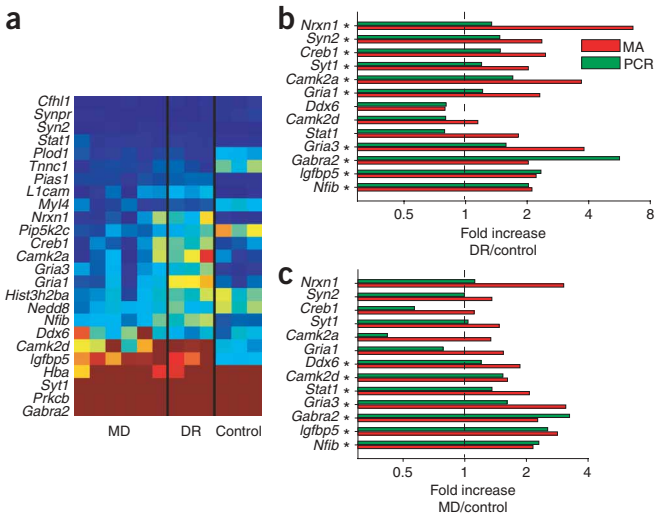

Figure 3 Confirmation of selected genes with RT-PCR. (**a**) Heat map of the genes confirmed with semiquantitative PCR. The level of expression is represented in logarithmic scale; red corresponds to maximal expression and blue to minimal expression. The genes are ranked according to their expression level after MD. (**b**,**c**) Representation of the fold increase of selected genes after (**b**) DR or (**c**) MD versus control, for microarray expression levels (red) and PCR values (green). A star indicates that the microarray expression of the corresponding gene is significantly upregulated ($P < 0.05$) in DR versus control or MD versus control.

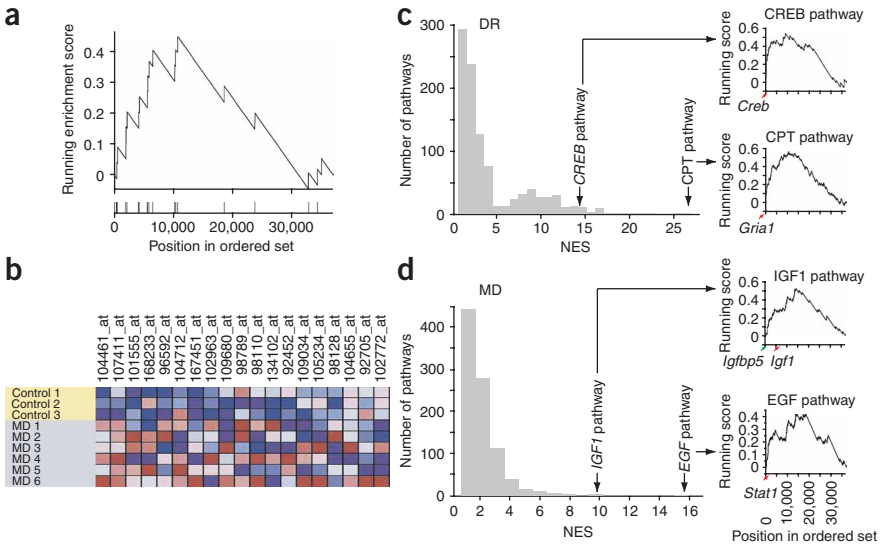

Figure 4 Gene set enrichment analysis of gene expression after DR and MD. (**a**) Example analysis of enrichment of the ARF pathway in the MD versus control dataset. The hypothesis tested was that the expression of the ARF gene set ($n = 19$ genes) is enriched in the MD versus control dataset. The genes in the ordered dataset are ranked according to their signal-to-noise ratio (see **Supplementary Methods**); upregulated genes appear first whereas downregulated genes appear late. Genes in the ranked list that are in the ARF pathway are marked on the abscissa (bottom). The running enrichment score is plotted in the graph (top). The peak enrichment score for the pathway is 0.48, leading to a normalized enriched score (NES) of 6.8. (**b**) Heat map of the expression levels of all probes of the ARF pathway gene set in the MD and control samples. (**c**) Distribution of NES values for the DR versus control dataset. The arrows highlight two pathways that are particularly enriched after DR: the CREB pathway and the channel passive transporter (CPT) pathway. Insets at right show the running enrichment scores for these two pathways; the red arrows show the positions of CREB and GluR1 probes, respectively. (**d**) Distribution of NES values for the MD versus control dataset. The arrows highlight the IGF1 and EGF pathways. The red arrows in the insets point to the positions of IGF1 and Stat1 probes, respectively, in the two pathways. The green arrow shows the location of the IGFBP5 probe in the MD dataset.

IGFBP5 and Nfib. Genes upregulated by long-term MD but not short-term MD included those for STAT1 and CaMKIIδ. Although some genes associated with synaptic transmission (such as those encoding GluR1, GluR3 and $GABA_A\alpha 2$) did not change after short-term MD, many more transmission-related genes (such as those encoding synapsin-2 and synaptotagmin-1) were up- or downregulated after short-term compared to long-term MD.

Gene set enrichment analysis

Apart from the expression of individual genes, sets of genes that are linked together in specific functional pathways may be differentially expressed after DR or MD and thereby lead to different cellular and molecular responses following the two forms of deprivation. To examine this possibility, we used a computational tool—gene set enrichment analysis (GSEA)—that considers the activation of sets of genes (such as genes underlying cellular pathways, coexpressed genes or genes in the same genomic locus) rather than the expression of a single transcript[23]. We were thus able to measure the extent to which a set of genes or a pathway is enriched in the deprivation protocols with respect to control (or vice versa). We considered 1,374 pathways and gene sets taken from a number of databases (the full list is available at http://web.mit.edu/msur/www/Tropea.html). An example of the computation of the enrichment score (**Supplementary Methods**) is shown for the ADP ribosylation factor (ARF) pathway (**Fig. 4a**). Qualitatively, most of the 19 probes for this

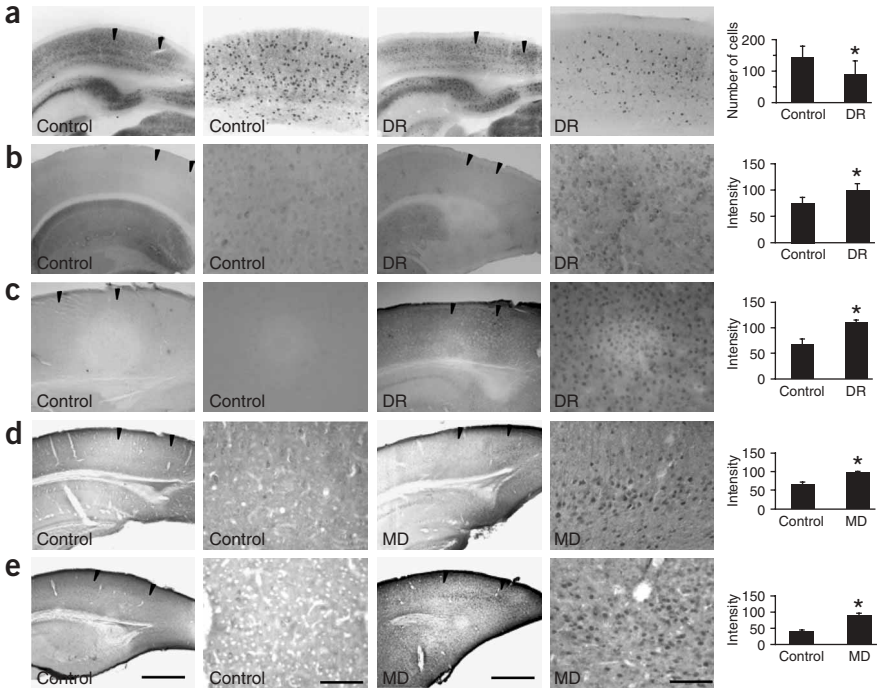

Figure 5 Protein expression analyses of selected molecules after DR and MD. Immunohistochemistry was performed on coronal slices containing V1 from P27 control, DR and MD mice. In DR mice, the expression of three proteins, parvalbumin, GluR1 and phospho-CREB, was examined. (**a**) Parvalbumin-expressing neurons are reduced in DR mice relative to control. The decrease in number is significant (indicated by star; $P < 0.01$) as shown in the histogram at right. (**b**) GluR1 and (**c**) phospho-CREB have increased expression in DR mice. Bars in the right histograms show that the intensity of staining was significantly greater ($P < 0.05$) in DR mice than in controls. (**d**,**e**) In MD mice, the expression of activated Stat1 (**d**) and IGFBP5 (**e**) is significantly increased ($P < 0.05$), relative to control, after 15 d of MD. For each molecule, low-magnification (scale bar 765 μm) and high-magnification panels (scale bar 100 μm) are shown. Arrows in the low-magnification panels demarcate V1. Error bars in histograms denote s.e.m.

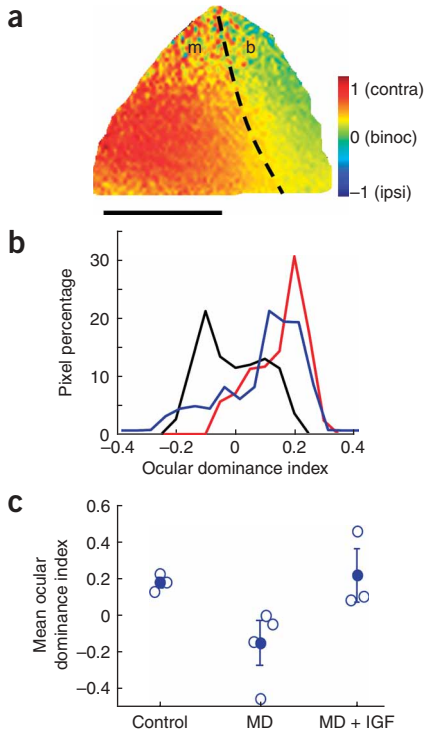

Figure 6 Application of IGF1 prevents the ocular dominance shift after MD in mouse V1. (**a**) Ocular dominance map in mouse V1. The dotted line separates the binocular zone (b) from the monocular zone (m). Color key at right depicts the binocularity index of pixels (**Supplementary Methods**). Scale bar, 1 mm. (**b**) Ocular dominance index histograms from the binocular zone of three representative mice. Red line, P27 control mouse; black line, P27 mouse after 7 d of MD; blue line, P30 mouse after 7 d of MD plus IGF1 application for the same period. The data from each mouse include a region within binocular cortex containing over 2,000 pixels. (**c**) Mean ocular dominance indices of the three groups of mice. Open circles, mean ocular dominance index of the binocular zone histograms from each mouse; filled circles, average value of each group.

pathway were more highly expressed after MD than in control (**Fig. 4b**). Quantitatively, many of these probes were highly ranked in the ordered set of MD probes (**Fig. 4a**), leading to a high running enrichment score for the ARF pathway. The gene sets with the highest scores in the deprived conditions as compared to control (**Supplementary Table 3**), and the gene sets with the highest scores in the control as compared to deprived conditions (that is, downregulated after deprivation; **Supplementary Table 4** online), were all significantly enriched (permutation test, $P < 0.0001$) within the dataset. The GSEA method revealed quantitatively that different gene sets were preferentially activated after DR and MD. For example, the top enriched gene sets after DR included those involved in cellular activity, encompassing both pathways related to metabolism (such as 'metabolism' and 'growth hormone pathway') and networks related to synaptic activity (such as 'channel passive transporter', 'vesicle-coat-protein' and 'secretory vesicles'). After MD, however, the majority of the top enriched gene sets corresponded to pathways activated by growth factors ('epidermal growth factor', 'insulin-like growth factor 1' and 'platelet derived growth factor') and neuronal remodeling and degeneration ('nuclear factor of activated T cells', 'JAK-STAT cascade' and 'embryogenesis and morphogenesis'). Several gene sets were enriched in both conditions but were ranked in a different order (**Supplementary Table 3**), confirming that common processes are also shared between the two conditions.

Notably, the genes we previously identified by RT-PCR as highly expressed after DR or MD were also present in specific gene sets with high normalized enriched score (NES) values (corresponding gene sets are marked in **Supplementary Table 2**), indicating that highly expressed genes together enrich specific pathways or networks of activation. The distribution of positive NES values for the DR versus control comparison (**Fig. 4c**) also shows the running enrichment scores for two pathways containing the molecules CREB and GluR1, respectively. The NES distribution for the MD versus control comparison (**Fig. 4d**) shows the running enrichment scores for two pathways containing the molecules STAT1 and IGF1/IGFBP5, respectively. Each of these genes appears early in the rank-ordered set of DR or MD genes (that is, it is one of the top enriched genes in the set and contributes significantly to the running enrichment score shown in **Fig. 4c**,**d**). Indeed, individual pathways often contain a number of key genes that are implicated in DR or MD. Conversely, individual genes are often included in multiple pathways enriched after DR or MD. Many genes are common between the two deprivation conditions, as expected, but several are different (compare **Fig. 3**). Considering the 100 gene sets most enriched under deprivation conditions, 1,928 probes are present in DR but not MD gene sets, 1,590 probes are present in MD but not DR gene sets, and 2,361 probes are present in both MD and DR gene sets.

Protein expression analysis of molecules and pathways

The results described thus far represent information at the mRNA level. We subsequently analyzed the expression of particular proteins using immunohistochemistry. We first examined markers for selected classes of interneurons. Because all the microarray probes for parvalbumin were downregulated after DR (**Fig. 2b**) while other interneuron markers remained unchanged or increased, we asked whether a similar pattern was reflected in the number of neurons that were immunopositive for these markers. We found a significant decrease (by 40%, $P < 0.01$) in the number of parvalbumin-positive neurons in DR relative to control mice (**Fig. 5a**), whereas calretinin-positive neurons remained unaltered and the number of neurons positive for somatostatin and neuropeptide Y increased ($P < 0.05$; **Supplementary Fig. 3** online). There was no effect of MD on the number of stained neurons for any of the antibodies examined. Thus, a key consequence of DR is a delay in the development of neurons that specifically express parvalbumin.

Following up on the gene sets highly enriched after DR, we examined the expression of GluR1 (**Fig. 5b**) and phospho-CREB (**Fig. 5c**), as well as CaMKIIα (data not shown), present in the 'CREB pathway' gene set. Each of these molecules was overexpressed in V1 of DR mice as compared to control, consistent with previous reports of the involvement of CaMKIIα in DR[24], of GluR1 as a substrate for CaMKIIα expression[25] and of CREB-mediated gene expression as related to the maturation of the visual cortex[26]. Similarly, after MD, we examined two novel proteins, activated STAT1 and IGFBP5, which are constituents of highly enriched gene sets, though neither has been previously implicated in the cortical effects of MD or any form of visual deprivation. STAT proteins are phosphorylated by Janus kinases (JAK); the JAK-STAT cascade is usually activated in response to cytokine signaling, but it is also upregulated in response to nerve injury and ischemia[27]. Immunostaining for the phosphorylated form of STAT1, indicating activation of the JAK-STAT cascade, showed that the molecule was significantly upregulated in V1 after MD (**Fig. 5d**). IGFBP5 is widely expressed in the brain[28] and binds IGF1, a peptide that is genetically

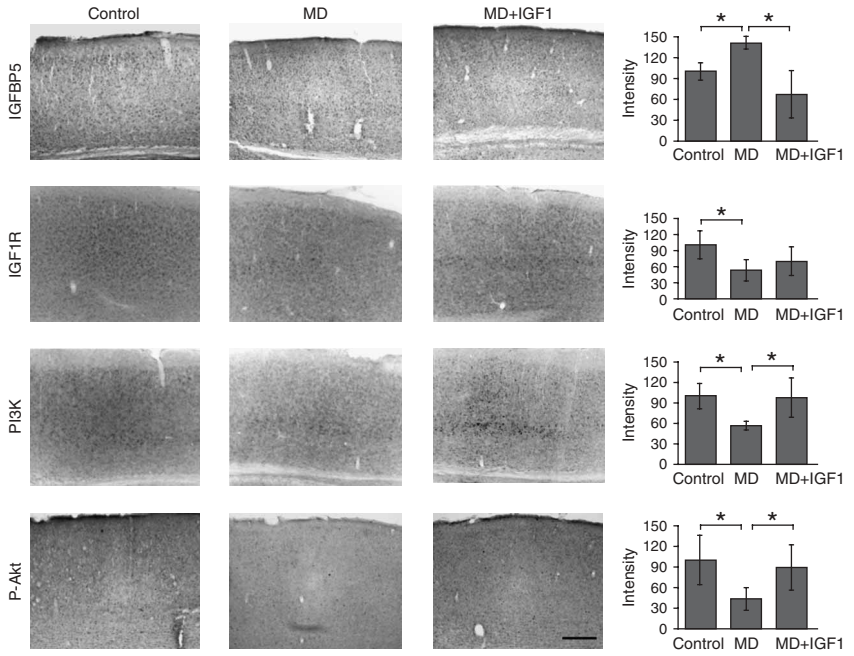

Figure 7 Immunohistochemistry studies for selected markers of the IGF1 pathway. Immunostaining for IGFBP5, the IGF1 receptor IGF1R, phosphatidylinositol kinase-3 (PI3K) and phosphorylated Akt (P-Akt) in three different conditions: P28 control (mice reared in normal light conditions), P28 MD (mice monocularly deprived for 4 d) and P28 MD+IGF1 (mice deprived for 4 d and simultaneously injected i.p. daily with IGF1 solution). In the MD panels, the cortex shown is contralateral to the deprived eye. Scale bar at bottom right, 70 μm; applies to all panels. Histograms at right show the staining intensity of each molecule in the different conditions. Star indicates a significant change ($P < 0.05$). Error bars denote s.e.m.

related to insulin[29] and is a potential mediator of cortical reorganization[30,31]. We found that IGFBP5 expression was significantly upregulated in V1 after long-term MD (**Fig. 5e**).

IGF1 pathway and ocular dominance plasticity

IGFBP5 is one of the genes most upregulated after MD, with a very high signal-to-noise ratio of microarray expression, one of the highest mRNA expression levels after RT-PCR, and the highest differential level of protein expression after MD or DR. Furthermore, the IGF1 pathway is one of the pathways most highly enriched after MD in the GSEA, and several of its probes are constituents of other pathways that are highly enriched after MD. We reasoned that the upregulation of IGFBP5 after MD could imply a competitive role for IGF1 in mediating ocular dominance plasticity after MD, and that exogenous application of IGF1 could then prevent the effect of MD (see, for example, ref. 32). The possible functional involvement of the IGF1-IGFBP5 system in experience-dependent plasticity in visual or any cortex has not been examined to date. We thus tested *in vivo* the physiological effects of IGF1 administration on ocular dominance plasticity in V1 (**Fig. 6**).

We took advantage of the fact that IGF1 is able to cross the blood-brain barrier: intraperitoneal (i.p.) administration of IGF1 prevents the effects of ischemia in the CNS[33]. We used optical imaging of intrinsic signals to evaluate the strength of signals from each eye in the physiologically identified binocular portion of V1 (**Fig. 6a**). Imaging was performed on three age-matched groups of mice during the critical period: control mice ($n = 3$), mice monocularly deprived for 7 d ($n = 4$) and MD mice with IGF1 delivered i.p. daily during the period of deprivation ($n = 3$). The ocular dominance distribution of pixels within the binocular zone in a control mouse (**Fig. 6b**) indicated that the pixel distribution favored the contralateral eye, as described previously with electrophysiological recordings[17]. Suturing the contralateral eye caused the ocular dominance distribution to shift toward the open, ipsilateral eye. Simultaneous administration of IGF1 prevented the ocular dominance shift toward the open eye (**Fig. 6b**). A comparison of the mean ocular dominance index across the population of mice (**Fig. 6c**) showed that deprivation of the contralateral eye shifted the index significantly relative to control mice ($P < 0.05$, treating each mouse as a single datum), whereas MD combined with administration of IGF1 prevented the shift ($P > 0.2$).

We investigated the mechanisms of IGF1 and IGFBP5 action by asking whether specific cell types and proteins were associated with the pathway. To clarify whether IGFBP5 is expressed in excitatory or inhibitory neurons, we performed a double immunostaining for IGFBP5 and GAD67 and found that IGFBP5 is expressed in a range of neurons—not exclusively in inhibitory interneurons (**Supplementary Fig. 4** online). Next we assayed, by immunostaining, the expression in V1 of several molecules involved in IGF1 signaling[29] both after MD alone and after MD with concurrent delivery of IGF1 (**Fig. 7**). IGFBP5 immunostaining showed a significant increase after short-term MD, and no change from normal levels in short-term MD mice that also received IGF1 during the deprivation period (MD+IGF1). Expression of the IGF1 receptor (IGF1R), on the other hand, was significantly downregulated after MD, and expression was partially restored in MD+IGF1-treated mice. PI3K, which is activated by IGF1, was significantly diminished in expression after MD but was fully restored after MD+IGF1 treatment ($P < 0.05$ for both comparisons; **Fig. 7**). Expression of one of the substrates of PI3K, phosphorylated Akt, was significantly reduced by MD and restored by addition of IGF1. Because IGF1 and PI3K signaling have been related to neuronal transmission[34], we screened for changes in synaptic activity by immunostaining for synapsin 1. The level of synapsin expression did not change significantly in MD mice as compared to control, but MD+IGF1 mice showed a significant increase ($P < 0.05$; data not shown). Finally, we performed a microarray analysis of MD+IGF1 mice for comparison with MD mice, to examine genes that might be differentially regulated by IGF1 and hence be associated specifically with IGF1 mechanisms (**Supplementary Fig. 5** online). Expression of only a small fraction of genes was significantly altered in MD+IGF1 mice as compared to MD mice (**Supplementary Table 2**; the entire gene list is available on the website). Notably, adding IGF1 significantly downregulated IGFBP5 and upregulated PI3K compared to MD alone ($P < 0.01$). Thus, PI3K appears to be an important signal downstream of IGF1 in mediating ocular dominance plasticity.

DISCUSSION

We used DNA microarrays to examine gene expression profiles in V1 in control mice and in mice reared under two conditions of visual input deprivation, DR and MD. The cortex was examined at P27, in a

protocol chosen to highlight similarities and differences among these conditions at the peak of the critical period[17]. RT-PCR analyses with independent samples confirmed the gene expression levels found with the microarray screen. We also confirmed the changes at the protein level for selected key molecules. Analysis of the expression of individual genes and gene sets, and of pathways that were up- or downregulated after DR or MD, led to several new conclusions. The delay in cortical maturation after DR is likely to be related to a decrease in parvalbumin expression and in parvalbuminergic neurons, as other interneuron markers or synaptic transmission–related genes do not change, or even increase, in both RNA and protein expression levels. In DR, the highly enriched gene sets point to a general increase in pathways related to synaptic and neuronal activity, which is consistent with the results obtained from a GO classification for individual genes, from expression levels of individual excitatory and inhibitory receptors, and from RT-PCR analysis of individual activity-related molecules. In MD, by contrast, there is enrichment of pathways mediated by growth factors and of pathways putatively involved in neuronal reorganization, response to injury or neurodegeneration. Although the role of growth factors in ocular dominance plasticity induced by MD has been described[35], the involvement of new pathways and their associated molecules, such as STAT1 and IGF1/IGFBP5, had not been suspected; these were confirmed by protein expression and, in the case of IGF1, by *in vivo* physiological studies. Analysis of IGF1 action at the protein and RNA levels suggests that this growth factor has a role in ocular dominance plasticity through the activation of PI3K.

Considerable evidence supports a sequence of signals that accompanies functional ocular dominance plasticity after MD[2]. NMDA receptors[36,37] and a critical level of inhibition[38] are required to detect an imbalance of inputs from the two eyes. Subsequently, signaling by PKA, CaMKII and ERK is required to initiate functional changes at synapses, including long-lasting changes that require protein synthesis, activation of CREB and production of brain-derived neurotrophic factor (BDNF). The structural correlates of ocular dominance plasticity, by contrast, are just beginning to be understood. A key step is the activation of proteases, including tissue plasminogen activator (tPA), that cleave the extracellular matrix[11,39,40], leading to alteration of spine dynamics of V1 neurons[11]. The mechanisms that cause deprived eye axons to withdraw and non-deprived eye axons to expand[12,13] are unknown. MD selectively upregulates a few genes associated with glutamatergic transmission (including those encoding NR1, GluR2 and GluR3; **Supplementary Fig. 1**), but most of the molecules above are not significantly up- or downregulated by MD in our microarray screen. This is not unexpected, for the functional effects of MD simply require the presence of these molecules during the critical period rather than their regulation by activity. Similarly, although the α1 subunit of the $GABA_A$ receptor is implicated in functional ocular dominance plasticity[41], the expression of this molecule is also not significantly altered by MD.

The functional effects of DR, by contrast, suggest a delay of the critical period, possibly through a delay in the onset of inhibition and a concomitant change in the threshold for eliciting synaptic plasticity (discussed above). We demonstrate here for the first time the specific and possibly exclusive involvement of parvalbumin-expressing interneurons in this function. Both the expression of parvalbumin RNA and the number of parvalbumin-stained cells are significantly decreased in DR mice. This is consistent with the hypothesis that development of parvalbumin expressing neurons is associated with the critical period[42]. Moreover, parvalbuminergic neurons are the principal inputs for postsynaptic receptors enriched in $GABA_A$ α1 subunits[41], suggesting that the upregulation of this subunit in DR but not in MD animals is a compensatory response to the development of parvalbuminergic circuitry.

Equally important, DR upregulates genes for a wide range of glutamatergic and GABAergic receptors, along with a number of signaling molecules such as CaMKIIα that lie downstream of synaptic activity and intracellular calcium entry. These findings are consistent with the proposal that neurons try to preserve a certain level of input drive and cellular signaling and adjust their synaptic and signaling mechanisms adaptively to the ongoing level of drive to maintain a balance between excitation and inhibition[8]. The regulation of a wide range of genes in DR, including those for excitation and inhibition, can be expected to have functional consequences. One hypothesis is that the upregulation of genes involved in excitatory transmission may increase the background level of activity in DR cortex compared to normal, whereas the upregulation of inhibition-related genes may reduce visually driven activity. Indeed, the observed increase in the amplitude of miniature excitatory postsynaptic potentials in V1 neurons after DR compared to normal is consistent with an increase in background activity in DR cortex[3]. Visually driven activity is reduced relative to background in DR ferrets[43], a fact we have confirmed in DR mice: the amplitude of the optical signal at the fundamental frequency of the stimulus is significantly lower in DR mice than in age-matched controls (control, 5.1 ± 1 units; DR, 1.4 ± 0.3 units; $n = 3$ mice each; $P < 0.05$). These data raise the possibility that the reduction of response amplitude is mediated by upregulation of specific interneuron classes (**Supplementary Fig. 3**; though we cannot rule out a reduction of presynaptic mechanisms), whereas the prolongation of plasticity is due to delayed maturation of neurons that express parvalbumin.

Computational analyses of gene sets indicate quantitatively the involvement of previously unsuspected pathways and molecules in mediating the effects of MD. Upregulation of the JAK-STAT cascade is complementary to findings in the LGN[44], showing that activity blockade in one eye with tetrodotoxin (TTX) produces a change in the expression level of RNAs encoding class I major histocompatibility complex (MHC) antigens. We did not find any change in expression of MHC molecules in our microarray screen, owing possibly to a difference either in the way deprivation was induced (eyelid suture versus intraocular TTX injection) or in the brain region investigated (cortex versus thalamus). Nonetheless, these results together suggest a role for cytokine related molecules in synaptic plasticity. Furthermore, JAK-STAT signaling is closely related to MAP kinase pathways[45], which are known to be central mediators of cortical ocular dominance plasticity[46].

IGFBP5 is one of the molecules most upregulated after MD with respect to both mRNA and protein expression, and it is included in the category of 'cellular physiological process' that is selectively present in MD (**Supplementary Table 1**). Exogenous application of its ligand, IGF1, prevents the functional ocular dominance shift that is a signature of MD. IGFBP5 increases the conversion of plasminogen into plasmin[47], and the associated cleavage of extracellular proteins exerts a key role in visual cortex plasticity[11,48]. The role of IGF1 in ocular dominance plasticity may be explained by several hypotheses[49]. First, it is possible that glucose metabolism has a significant role in mediating the effects of deprivation in visual cortex. IGF1 enhances glucose uptake[49] and may reduce deprivation-induced competition between afferents from the two eyes. In addition, IGF1 may function as a modulator of synaptic and neuronal activity and act like a subset of neurotrophins; indeed, its administration during MD recalls the effects of applying the neurotrophins nerve growth factor (NGF)[32] or neurotrophin-4 (NT4)[35] to visual cortex. BDNF and IGF1 are

overexpressed in V1 after retinal scotoma[31] and share components of their intracellular pathways (including PI3K)[30]. The last hypothesis is supported by our findings concerning the expression level of PI3K, which is selectively affected by MD and restored by exogenous application of IGF1.

Our findings point to coordinated sets of molecules and pathways that transduce input activity during development into cortical connectivity and function. Different forms of visual experience, such as DR and MD, activate some similar but also different mechanisms that underlie specific aspects of activity-dependent plasticity in visual cortex. The effects of DR indicate that sensory activity *per se* substantially regulates mechanisms associated with excitatory and inhibitory transmission. The effects of MD demonstrate that specific sensory experience additionally regulates mechanisms that adaptively match cortical connections to differential levels of input drive.

METHODS

RNA preparation and microarray analysis. Mice (129/SvEv) at the peak of the critical period[17], P27, were used. All animal protocols were approved by the Massachusetts Institute of Technology Committee on the Care and Use of Animals and followed US National Institutes of Health guidelines.

In a first set of experiments, we extracted total RNA from V1 of normally reared P27 mice (control, $n = 3$ samples), from V1 of P27 mice born and reared in darkness (DR, $n = 3$ samples), and from V1 contralateral to the deprived eye of P27 mice in which monocular deprivation was started at P11–12, before eye-opening (MD, $n = 6$ samples). (For MD, three samples were done with deprivation of the right eye and three with deprivation of the left eye; we considered these six samples as a group because we did not observe any difference between right- and left-eye deprivation.) For each sample, mice came from different litters and the tissue was derived from at least two different mice. In both groups of mice, monocular and binocular portions were included for analysis. Mice were anesthetized with phenobarbital (Nembutal; 100 mg/kg), decapitated, the skull opened, and a small core of tissue removed from the visual cortex. Total RNA was extracted and purified according to the instructions in the "Eukaryotic Target Preparation" manual available on the Affymetrix website. Fragmented, biotinylated cRNA was hybridized to the Affymetrix mouse genome U74v2 GeneChip set, which contains oligonucleotides that correspond to a total of 36,902 probes targeting genes and expressed sequence tags. The array processing (hybridization, washing, staining and scanning) was performed by the Biopolymer Laboratory at the Massachusetts Institute of Technology following standard Affymetrix protocols. A global scaling algorithm was used to normalize the expression level data from all samples. In additional experiments in which the effects of short-term (4 d from P23–27) MD were investigated, as well as the effects of IGF1 infusion concurrent with MD, we analyzed a total of four experimental groups: a new group of control mice (three samples), the ipsilateral and the contralateral cortex of mice monocularly deprived for 4 d (three samples for the ipsilateral and three samples for the contralateral cortex), and the contralateral cortex of mice that were monocularly deprived for 4 d and were injected i.p. daily with IGF1 solution (three samples). The tissue was removed and RNA extracted as above, and the labeled RNA was hybridized to the Affymetrix mouse genome 430.2 chip, which contains oligonucleotides that correspond to a total of 42,000 probes targeting genes and ESTs.

Data analysis. Significance analysis of microarrays was used to assess changes in gene expression. GO annotations were used in the first set of experiments to obtain information about the biological processes in which single genes are involved. FatiGO was used to identify categories for biological functions that are over- or under- represented in the different protocols of visual input deprivation. Detailed descriptions are given in **Supplementary Methods**.

To identify the mechanisms and pathways involved in experience-dependent development, we used a computational method, gene set enrichment analysis (GSEA), that considers the enrichment of sets of genes rather than the expression of a single transcript[23]. GSEA is a method for determining whether a rank-ordered list of genes for a particular comparison (for example, MD versus control; see **Fig. 4a**) has a rich representation of genes derived from an independently generated gene set (for example, genes representing a pathway or function).

We separately examined 1,374 gene sets derived from a number of databases. For each gene set, we plotted the running enrichment score as a function of the rank-ordered probes in the comparison set. We measured the maximum amplitude of deviation from 0 in the enrichment score and assessed the statistical significance of this deviation by a permutation test shuffling the gene labels. For each gene set, we also calculated an NES. A detailed description is provided in **Supplementary Methods**.

Semiquantitative RT-PCR. RNA was extracted as described above and cDNA was obtained with the Superscript First-Strand Synthesis System for RT-PCR (Invitrogen). PCR was carried out according to the Invitrogen instruction manual. For each sample, PCR was run for the genes encoding the selected molecules and glycerol phosphate dehydrogenase (GPDH) as a control. PCR products were stained with ethidium bromide and run on an agarose gel. The intensity of each band was evaluated with ImageJ software (http://rsb.info.nih.gov/ij/) and normalized by the level of GPDH gene expression.

Immunohistochemistry. Immunohistochemistry for GluR1 (1:500, Upstate Biotechnology), IGFBP5 (1:500, US Biological), CaMK2α (1:500, Sigma), phospho-CREB (1:500, Cell Signaling), activated Stat1 (1:500, Abcam), parvalbumin (1:1,000, Chemicon), calretinin (1:500, Chemicon), somatostatin (1:300, Chemicon), neuropeptide Y (1:400, Chemicon), synapsin 1 (1: 500, Chemicon), IGF1 (1:250, Chemicon), GAD 67 (1:400, Chemicon), IGF1R (1:500, Upstate Biotechnology), PI3K catalytic subunit 110 (1:400, Upstate Biotechnology), and phosphorylated Akt (1:250, Cell Signaling), was carried out on coronal sections[31,50]. Experiments were done in parallel for control and deprived mice, on at least two mice per group, and repeated twice. The intensity of staining in sections from control and deprived mice was evaluated with ImageJ software (http://rsb.info.nih.gov/ij/).

Optical imaging of V1. For optical imaging of intrinsic signals, mice (129/SvEv and C57Bl/6) aged P26–30 were anesthetized with urethane (1.5 g/kg) and chlorprothixene (0.2 mg). Detailed description of the surgical procedures, stimulus presentation and data analysis are provided in **Supplementary Methods**.

URLs and accession codes. Primary microarray data are available at GEO under the accession code GSE4537. Supplemental microarray and gene list information is available at http://web.mit.edu/msur/www/Tropea.html.

Note: Supplementary information is available on the Nature Neuroscience website.

ACKNOWLEDGMENTS

We thank members of the Sur lab for their assistance, comments and advice and the staff at the Massachusetts Institute of Technology BioMicro Center for processing the RNA samples and for advice on data analysis. Supported by a National Research Service Award fellowship from the US National Institutes of Health (D.T.), a McGovern Fellowship (G.K.) and grants from the NIH and the Simons Foundation (M.S.).

COMPETING INTERESTS STATEMENT

The authors declare that they have no competing financial interests.

Published online at http://www.nature.com/natureneuroscience
Reprints and permissions information is available online at http://npg.nature.com/reprintsandpermissions/

1. Sur, M. & Rubenstein, J.L. Patterning and plasticity of the cerebral cortex. *Science* **310**, 805–810 (2005).
2. Berardi, N., Pizzorusso, T., Ratto, G.M. & Maffei, L. Molecular basis of plasticity in the visual cortex. *Trends Neurosci.* **26**, 369–378 (2003).
3. Desai, N.S., Cudmore, R.H., Nelson, S.B. & Turrigiano, G.G. Critical periods for experience-dependent synaptic scaling in visual cortex. *Nat. Neurosci.* **5**, 783–789 (2002).
4. Wallace, W. & Bear, M.F. A morphological correlate of synaptic scaling in visual cortex. *J. Neurosci.* **24**, 6928–6938 (2004).
5. Kirkwood, A., Rioult, M.C. & Bear, M.F. Experience-dependent modification of synaptic plasticity in visual cortex. *Nature* **381**, 526–528 (1996).

6. Fagiolini, M., Pizzorusso, T., Berardi, N., Domenici, L. & Maffei, L. Functional postnatal development of the rat primary visual cortex and the role of visual experience: dark rearing and monocular deprivation. *Vision Res.* **34**, 709–720 (1994).
7. Morales, B., Choi, S.Y. & Kirkwood, A. Dark rearing alters the development of GABAergic transmission in visual cortex. *J. Neurosci.* **22**, 8084–8090 (2002).
8. Turrigiano, G.G. & Nelson, S.B. Homeostatic plasticity in the developing nervous system. *Nat. Rev. Neurosci.* **5**, 97–107 (2004).
9. Wiesel, T.N. & Hubel, D.H. Single-cell responses in striate cortex of kittens deprived of vision in one eye. *J. Neurophysiol.* **26**, 1003–1017 (1963).
10. Trachtenberg, J.T., Trepel, C. & Stryker, M.P. Rapid extragranular plasticity in the absence of thalamocortical plasticity in the developing primary visual cortex. *Science* **287**, 2029–2032 (2000).
11. Oray, S., Majewska, A. & Sur, M. Dendritic spine dynamics are regulated by monocular deprivation and extracellular matrix degradation. *Neuron* **44**, 1021–1030 (2004).
12. Antonini, A. & Stryker, M.P. Rapid remodeling of axonal arbors in the visual cortex. *Science* **260**, 1819–1821 (1993).
13. Shatz, C.J. & Stryker, M.P. Ocular dominance in layer IV of the cat's visual cortex and the effects of monocular deprivation. *J. Physiol. (Lond.)* **281**, 267–283 (1978).
14. Crowley, J.C. & Katz, L.C. Early development of ocular dominance columns. *Science* **290**, 1321–1324 (2000).
15. Prasad, S.S. *et al.* Gene expression patterns during enhanced periods of visual cortex plasticity. *Neuroscience* **111**, 35–45 (2002).
16. Ossipow, V., Pellissier, F., Schaad, O. & Ballivet, M. Gene expression analysis of the critical period in the visual cortex. *Mol. Cell. Neurosci.* **27**, 70–83 (2004).
17. Gordon, J.A. & Stryker, M.P. Experience-dependent plasticity of binocular responses in the primary visual cortex of the mouse. *J. Neurosci.* **16**, 3274–3286 (1996).
18. Majewska, A. & Sur, M. Motility of dendritic spines in visual cortex *in vivo:* changes during the critical period and effects of visual deprivation. *Proc. Natl. Acad. Sci. USA* **100**, 16024–16029 (2003).
19. Markram, H. *et al.* Interneurons of the neocortical inhibitory system. *Nat. Rev. Neurosci.* **5**, 793–807 (2004).
20. Abdelhaleem, M. Do human RNA helicases have a role in cancer? *Biochim. Biophys. Acta* **1704**, 37–46 (2004).
21. Murray, K.D., Isackson, P.J. & Jones, E.G. *N*-methyl-D-aspartate receptor dependent transcriptional regulation of two calcium/calmodulin-dependent protein kinase type II isoforms in rodent cerebral cortex. *Neuroscience* **122**, 407–420 (2003).
22. Steele-Perkins, G. *et al.* The transcription factor gene *Nfib* is essential for both lung maturation and brain development. *Mol. Cell. Biol.* **25**, 685–698 (2005).
23. Subramanian, A. *et al.* Gene set enrichment analysis: a knowledge-based approach for interpreting genome-wide expression profiles. *Proc. Natl. Acad. Sci. USA* **102**, 15545–15550 (2005).
24. Neve, R.L. & Bear, M.F. Visual experience regulates gene expression in the developing striate cortex. *Proc. Natl. Acad. Sci. USA* **86**, 4781–4784 (1989).
25. Xue, J., Li, G., Laabich, A. & Cooper, N.G. Visual-mediated regulation of retinal CaMKII and its GluR1 substrate is age-dependent. *Brain Res. Mol. Brain Res.* **93**, 95–104 (2001).
26. Pham, T.A., Impey, S., Storm, D.R. & Stryker, M.P. CRE-mediated gene transcription in neocortical neuronal plasticity during the developmental critical period. *Neuron* **22**, 63–72 (1999).
27. Justicia, C., Gabriel, C. & Planas, A.M. Activation of the JAK/STAT pathway following transient focal cerebral ischemia: signaling through Jak1 and Stat3 in astrocytes. *Glia* **30**, 253–270 (2000).
28. Iwadate, H., Sugisaki, T., Kudo, M. & Kizuki, K. Actions of insulin-like growth factor binding protein-5 (IGFBP-5) are potentially regulated by tissue kallikrein in rat brains. *Life Sci.* **73**, 3149–3158 (2003).
29. Bondy, C.A. & Cheng, C.M. Signaling by insulin-like growth factor 1 in brain. *Eur. J. Pharmacol.* **490**, 25–31 (2004).
30. Zheng, W.H. & Quirion, R. Comparative signaling pathways of insulin-like growth factor-1 and brain-derived neurotrophic factor in hippocampal neurons and the role of the PI3 kinase pathway in cell survival. *J. Neurochem.* **89**, 844–852 (2004).
31. Obata, S., Obata, J., Das, A. & Gilbert, C.D. Molecular correlates of topographic reorganization in primary visual cortex following retinal lesions. *Cereb. Cortex* **9**, 238–248 (1999).
32. Maffei, L., Berardi, N., Domenici, L., Parisi, V. & Pizzorusso, T. Nerve growth factor (NGF) prevents the shift in ocular dominance distribution of visual cortical neurons in monocularly deprived rats. *J. Neurosci.* **12**, 4651–4662 (1992).
33. Guan, J., Bennet, L., Gluckman, P.D. & Gunn, A.J. Insulin-like growth factor-1 and post-ischemic brain injury. *Prog. Neurobiol.* **70**, 443–462 (2003).
34. Blair, L.A. & Marshall, J. IGF-1 modulates N and L calcium channels in a PI 3-kinase-dependent manner. *Neuron* **19**, 421–429 (1997).
35. Lodovichi, C., Berardi, N., Pizzorusso, T. & Maffei, L. Effects of neurotrophins on cortical plasticity: same or different? *J. Neurosci.* **20**, 2155–2165 (2000).
36. Bear, M.F., Kleinschmidt, A., Gu, Q.A. & Singer, W. Disruption of experience-dependent synaptic modifications in striate cortex by infusion of an NMDA receptor antagonist. *J. Neurosci.* **10**, 909–925 (1990).
37. Roberts, E.B., Meredith, M.A. & Ramoa, A.S. Suppression of NMDA receptor function using antisense DNA block ocular dominance plasticity while preserving visual responses. *J. Neurophysiol.* **80**, 1021–1032 (1998).
38. Hensch, T.K. *et al.* Local GABA circuit control of experience-dependent plasticity in developing visual cortex. *Science* **282**, 1504–1508 (1998).
39. Pizzorusso, T. *et al.* Reactivation of ocular dominance plasticity in the adult visual cortex. *Science* **298**, 1248–1251 (2002).
40. Mataga, N., Nagai, N. & Hensch, T.K. Permissive proteolytic activity for visual cortical plasticity. *Proc. Natl. Acad. Sci. USA* **99**, 7717–7721 (2002).
41. Fagiolini, M. *et al.* Specific $GABA_A$ circuits for visual cortical plasticity. *Science* **303**, 1681–1683 (2004).
42. Huang, Z.J. *et al.* BDNF regulates the maturation of inhibition and the critical period of plasticity in mouse visual cortex. *Cell* **98**, 739–755 (1999).
43. White, L.E., Coppola, D.M. & Fitzpatrick, D. The contribution of sensory experience to the maturation of orientation selectivity in ferret visual cortex. *Nature* **411**, 1049–1052 (2001).
44. Corriveau, R.A., Huh, G.S. & Shatz, C.J. Regulation of class I MHC gene expression in the developing and mature CNS by neural activity. *Neuron* **21**, 505–520 (1998).
45. Xu, W., Nair, J.S., Malhotra, A. & Zhang, J.J. B cell antigen receptor signaling enhances IFN-γ-induced Stat1 target gene expression through calcium mobilization and activation of multiple serine kinase pathways. *J. Interferon Cytokine Res.* **25**, 113–124 (2005).
46. Di Cristo, G. *et al.* Requirement of ERK activation for visual cortical plasticity. *Science* **292**, 2337–2340 (2001).
47. Tonner, E. *et al.* Insulin-like growth factor binding protein-5 (IGFBP-5) potentially regulates programmed cell death and plasminogen activation in the mammary gland. *Adv. Exp. Med. Biol.* **480**, 45–53 (2000).
48. McGee, A.W., Yang, Y., Fischer, Q.S., Daw, N.W. & Strittmatter, S.M. Experience-driven plasticity of visual cortex limited by myelin and Nogo receptor. *Science* **309**, 2222–2226 (2005).
49. Bondy, C.A. & Cheng, C.M. Insulin-like growth factor-1 promotes neuronal glucose utilization during brain development and repair processes. *Int. Rev. Neurobiol.* **51**, 189–217 (2002).
50. Tropea, D., Caleo, M. & Maffei, L. Synergistic effects of brain-derived neurotrophic factor and chondroitinase ABC on retinal fiber sprouting after denervation of the superior colliculus in adult rats. *J. Neurosci.* **23**, 7034–7044 (2003).